The "wish to submit to PRC" CNAO 2017 paper

Data published on IEEE TRPMS (5/03/2020)

IlaMi from Milano and Roma

The Rationale of a Reanalysis

After 2020, FLUKA changes its policy to publish MC results. We decided to take our CNAO 2017 data and compare our results to the FLUKA MC predictions.
In order to do so, we had (and had the opportunity) to refine the analysis:

- **improvement on the evaluation of the kinetic energy at production**: unfolding technique instead of analytical evaluation
- **improvement of the particle identification efficiency**: not averaged but binned in kinetic energy at production
- **improvement on the systematic error evaluation** (and MC closure test done to assess the reliability of the computed efficiencies)

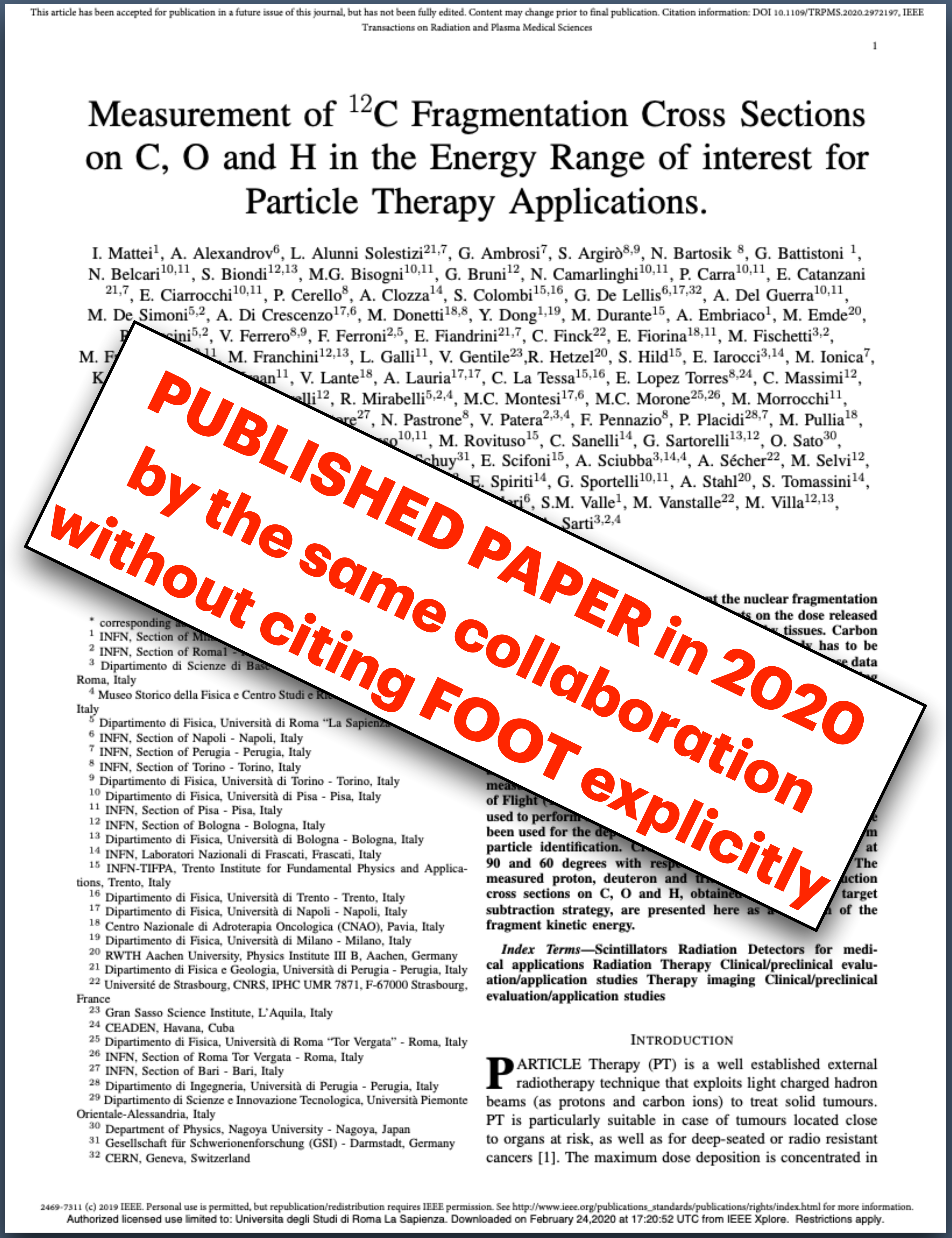

This article has been accepted for publication in a future issue of this journal, but has not been fully edited. Content may change prior to final publication. Citation information: DOI 10.1109/TRPMS.2020.2972197, IEEE Transactions on Radiation and Plasma Medical Sciences

1

Measurement of ^{12}C Fragmentation Cross Sections on C, O and H in the Energy Range of interest for Particle Therapy Applications.

I. Mattei[1], A. Alexandrov[6], L. Alunni Solestizi[21,7], G. Ambrosi[7], S. Argirò[8,9], N. Bartosik [8], G. Battistoni [1], N. Belcari[10,11], S. Biondi[12,13], M.G. Bisogni[10,11], G. Bruni[12], N. Camarlinghi[10,11], P. Carra[10,11], E. Catanzani [21,7], E. Ciarrocchi[10,11], P. Cerello[8], A. Clozza[14], S. Colombi[15,16], G. De Lellis[6,17,32], A. Del Guerra[10,11], M. De Simoni[5,2], A. Di Crescenzo[17,6], M. Donetti[18,8], Y. Dong[1,19], M. Durante[15], A. Embriaco[1], M. Emde[20], ...cini[5,2], V. Ferrero[8,9], F. Ferroni[2,5], E. Fiandrini[21,7], C. Finck[22], E. Fiorina[18,11], M. Fischetti[3,2], ... M. Franchini[12,13], L. Galli[11], V. Gentile[23], R. Hetzel[20], S. Hild[15], E. Iarocci[3,14], M. Ionica[7], ...an[11], V. Lante[18], A. Lauria[17,17], C. La Tessa[15,16], E. Lopez Torres[8,24], C. Massimi[12], ...lli[12], R. Mirabelli[5,2,4], M.C. Montesi[17,6], M.C. Morone[25,26], M. Morrocchi[11], ...re[27], N. Pastrone[8], V. Patera[2,3,4], F. Pennazio[8], P. Placidi[28,7], M. Pullia[18], ...o[10,11], M. Rovituso[15], C. Sanelli[14], G. Sartorelli[13,12], O. Sato[30], ...chuy[31], E. Scifoni[15], A. Sciubba[3,14,4], A. Sécher[22], M. Selvi[12], ... E. Spiriti[14], G. Sportelli[10,11], A. Stahl[20], S. Tomassini[14], ...ri[6], S.M. Valle[1], M. Vanstalle[22], M. Villa[12,13], ... Sarti[3,2,4]

* corresponding ...
[1] INFN, Section of Mi...
[2] INFN, Section of Roma1 ...
[3] Dipartimento di Scienze di Bas... Roma, Italy
[4] Museo Storico della Fisica e Centro Studi e Ri... Italy
[5] Dipartimento di Fisica, Università di Roma "La Sapienza...
[6] INFN, Section of Napoli - Napoli, Italy
[7] INFN, Section of Perugia - Perugia, Italy
[8] INFN, Section of Torino - Torino, Italy
[9] Dipartimento di Fisica, Università di Torino - Torino, Italy
[10] Dipartimento di Fisica, Università di Pisa - Pisa, Italy
[11] INFN, Section of Pisa - Pisa, Italy
[12] INFN, Section of Bologna - Bologna, Italy
[13] Dipartimento di Fisica, Università di Bologna - Bologna, Italy
[14] INFN, Laboratori Nazionali di Frascati, Frascati, Italy
[15] INFN-TIFPA, Trento Institute for Fundamental Physics and Applications, Trento, Italy
[16] Dipartimento di Fisica, Università di Trento - Trento, Italy
[17] Dipartimento di Fisica, Università di Napoli - Napoli, Italy
[18] Centro Nazionale di Adroterapia Oncologica (CNAO), Pavia, Italy
[19] Dipartimento di Fisica, Università di Milano - Milano, Italy
[20] RWTH Aachen University, Physics Institute III B, Aachen, Germany
[21] Dipartimento di Fisica e Geologia, Università di Perugia - Perugia, Italy
[22] Université de Strasbourg, CNRS, IPHC UMR 7871, F-67000 Strasbourg, France
[23] Gran Sasso Science Institute, L'Aquila, Italy
[24] CEADEN, Havana, Cuba
[25] Dipartimento di Fisica, Università di Roma "Tor Vergata" - Roma, Italy
[26] INFN, Section of Roma Tor Vergata - Roma, Italy
[27] INFN, Section of Bari - Bari, Italy
[28] Dipartimento di Ingegneria, Università di Perugia - Perugia, Italy
[29] Dipartimento di Scienze e Innovazione Tecnologica, Università Piemonte Orientale-Alessandria, Italy
[30] Department of Physics, Nagoya University - Nagoya, Japan
[31] Gesellschaft für Schwerionenforschung (GSI) - Darmstadt, Germany
[32] CERN, Geneva, Switzerland

...t the nuclear fragmentation ...ts on the dose released ... tissues. Carbon ... has to be ... data ... measu... of Flight ... used to perform ... been used for the de... particle identification. C... at 90 and 60 degrees with resp... The measured proton, deuteron and tr... uction cross sections on C, O and H, obtained ... target subtraction strategy, are presented here as a ... of the fragment kinetic energy.

Index Terms—Scintillators Radiation Detectors for medical applications Radiation Therapy Clinical/preclinical evaluation/application studies Therapy imaging Clinical/preclinical evaluation/application studies

INTRODUCTION

PARTICLE Therapy (PT) is a well established external radiotherapy technique that exploits light charged hadron beams (as protons and carbon ions) to treat solid tumours. PT is particularly suitable in case of tumours located close to organs at risk, as well as for deep-seated or radio resistant cancers [1]. The maximum dose deposition is concentrated in

Title and Authors

Cross Section Measurements of Large Angle Fragments Production in the Interaction of Carbon Ion Beams with Thin Targets

Y. Dong,[1] I. Mattei,[1] A. Alexandrov,[2] B. Alpat,[3] G. Ambrosi,[3] S. Argirò,[4, 5] M. Barbanera,[3] N. Bartosik,[5] G. Battistoni,[1] M.G. Bisogni,[6, 7] V. Boccia,[8, 2] F. Cavanna,[5] P. Cerello,[5] E. Ciarrocchi,[6, 7] A. De Gregorio,[9, 10] G. De Lellis,[8, 2] A. Di Crescenzo,[8, 2] B. Di Ruzza,[11] M. Dondi,[12, 13] M. Donetti,[14, 5] M. Durante,[8, 15] R. Faccini,[9, 10] V. Ferrero,[5] C. Finck,[16] E. Fiorina,[5] M. Francesconi,[2] M. Franchini,[12, 13] G. Franciosini,[17, 10] G. Galati,[18] L. Galli,[7] M. Ionica,[3] A. Iuliano,[8, 2] K. Kanxheri,[3, 19] A.C. Kraan,[7] C. La Tessa,[20, 21] A. Lauria,[8, 2] E. Lopez Torres,[22, 5] M. Magi,[17, 10] A. Manna,[13, 12] M. Marafini,[23, 10] M. Massa,[7] C. Massimi,[12, 13] A. Mengarelli,[13] A. Mereghetti,[14] T. Minniti,[24, 25] A. Moggi,[7] M.C. Montesi,[2, 26] M.C. Morone,[24, 25] M. Morrocchi,[6, 7] S. Muraro,[1] N. Pastrone,[5] V. Patera,[17, 10] F. Peverini,[3, 19] F. Pennazio,[5] C. Pisanti,[12, 13] P. Placidi,[3, 27] M. Pullia,[14] L. Ramello,[5, 28] C. Reidel,[15] R. Ridolfi,[13, 12] L. Sabatini,[29] L. Salvi,[3, 19] C. Sanelli,[29] A. Sarti,[17, 10] O. Sato,[30] S. Savazzi,[14] L. Scavarda,[31] A. Schiavi,[17, 10] C. Schuy,[15] E. Scifoni,[21] L. Servoli,[3] G. Silvestre,[3] M. Sitta,[5, 32] R. Spighi,[13] E. Spiriti,[29] L. Testa,[9, 7] V. Tioukov,[2] S. Tomassini,[29] F. Tommasino,[33, 21] M. Toppi,[17, 10] A. Trigilio,[29] G. Traini,[10] G. Ubaldi,[12, 13] A. Valetti,[4, 5] M. Vanstalle,[16] U. Weber,[15] R. Zarrella,[12, 13] A. Zoccoli,[12, 13] and M. Villa[12, 13]

Title is long, made by keywords.

Author list provided by the EB.

Abstract

The fragmentation cross sections of carbon ion beams with a kinetic energy of 115 – 353 MeV/u impinging on thin targets of graphite (C), PMMA ($C_2O_5H_8$) and polyvinyl-toluene (C_9H_{10}) have been measured at 90° and 60° at the CNAO particle therapy center (Pavia, Italy). Cross sections on elemental targets exploiting the target subtraction method have already been published[1]. The presented measurement is a complete reanalysis by the FOOT collaboration[2] of the already published data on composite targets, in order to refine the analysis, improve the systematic uncertainties and show the comparison with the FLUKA Monte Carlo code calculations. In this work, the kinetic energy at production of measured fragments has been completely redefined, together with the efficiencies computation. The new analysis strategy has been successfully validated against the true MC cross sections. Two detection arms were positioned at two different angles to perform the measurement at 90° and 60°. The fragment species has been identified in charge (Z_{id} = H, He) and mass (M_{id} = ^{1}H, ^{2}H, ^{3}H) combining the information of the deposited energy in thin plastic scintillators, of the deposited energy in a thick LYSO crystal and of the fragments Time of Flight (ToF) measurement. The ToF was also used to compute the fragments measured kinetic energy. The cross sections are presented as a function of the fragments production kinetic energy thanks to an unfolding technique applied to data.

We can't avoid saying that this is a reanalysis. There are already published data on the same dataset.

Introduction

INTRODUCTION

Particle Therapy (PT) is the external radiation therapy technique that exploits protons and carbon ion beams to treat especially deep-seated solid tumors close to organs at risk[3]. In particular, carbon ions are used to treat radio-resistant tumors thanks to their higher biological effectiveness in killing cancerous cells with respect to photons and protons[4], but hadrons with a mass number $A > 1$ may undergo fragmentation in the nuclear interaction

Background and measurement motivation.

Motivation of the reanalysis and description of the paper Sections.

The experimental data of the cross section of ^{12}C ion beam on carbon (C), oxygen (O) and hydrogen (H) elemental targets at large angle have been already published[1] by the FOOT collaboration[2], exploiting the composite targets subtraction method from the cross section of ^{12}C ion beam impinging on C, CH and PMMA targets, from a data taking performed at the CNAO therapy center (Pavia, Italy). In this work a reanalysis of the same dataset is performed, motivated by an improvement in the whole analysis strategy, in particular in the efficiency computation, in the extraction of the kinetic energy through a new unfolding technique and in the systematic uncertainties evaluation. In Section I the experimental setup and configurations are described, in Section II the data analysis strategy is presented. The computation of the fragment kinetic energy at production has been implemented exploiting an unfolding technique of the measured fragment kinetic energy (see Section II A 1), while in the already published data an analytic function was applied for the measured kinetic energy correction. Moreover, instead of computing a fragment identification efficiency averaged on the kinetic energy at production of fragments, in the presented analysis the fragment identification efficiency is modulated as a function of the fragment production kinetic energy (see Section II B 2). The systematic error evaluation has been discussed in Section II C. In Section III the results are reported and the comparison with FLUKA Monte Carlo code[12,13] predictions is also shown for the first time and discussed in Section IV.

Section I: Experimental Configurations

I. EXPERIMENTAL CONFIGURATIONS

The double differential fragmentation cross sections of ^{12}C ion beam over C, CH and PMMA thin targets (see Table I) have been measured, exploiting five beam energies: 115 MeV/u, 150 MeV/u, 221 MeV/u, 279 MeV/u and 351 MeV/u. The beam intensity was the therapeutical one ($\sim 10^8$ ions/s). Each target, placed at 45° with respect to the incoming beam direction ($th_Y = Thickness \cdot \sqrt{2}$), was impinged by $\sim 5 \cdot 10^{10}$ ions.

Target	Composition	Thickness [mm]	th_Y [mm]	Density [g/cm^3]
PMMA	$C_5O_2H_8$	2	2.8	1.19
Graphite	C	1	1.4	0.94
Polyvinyl-toluene	C_9H_{10}	2	2.8	1.024

TABLE I. Targets composition and parameters[1].

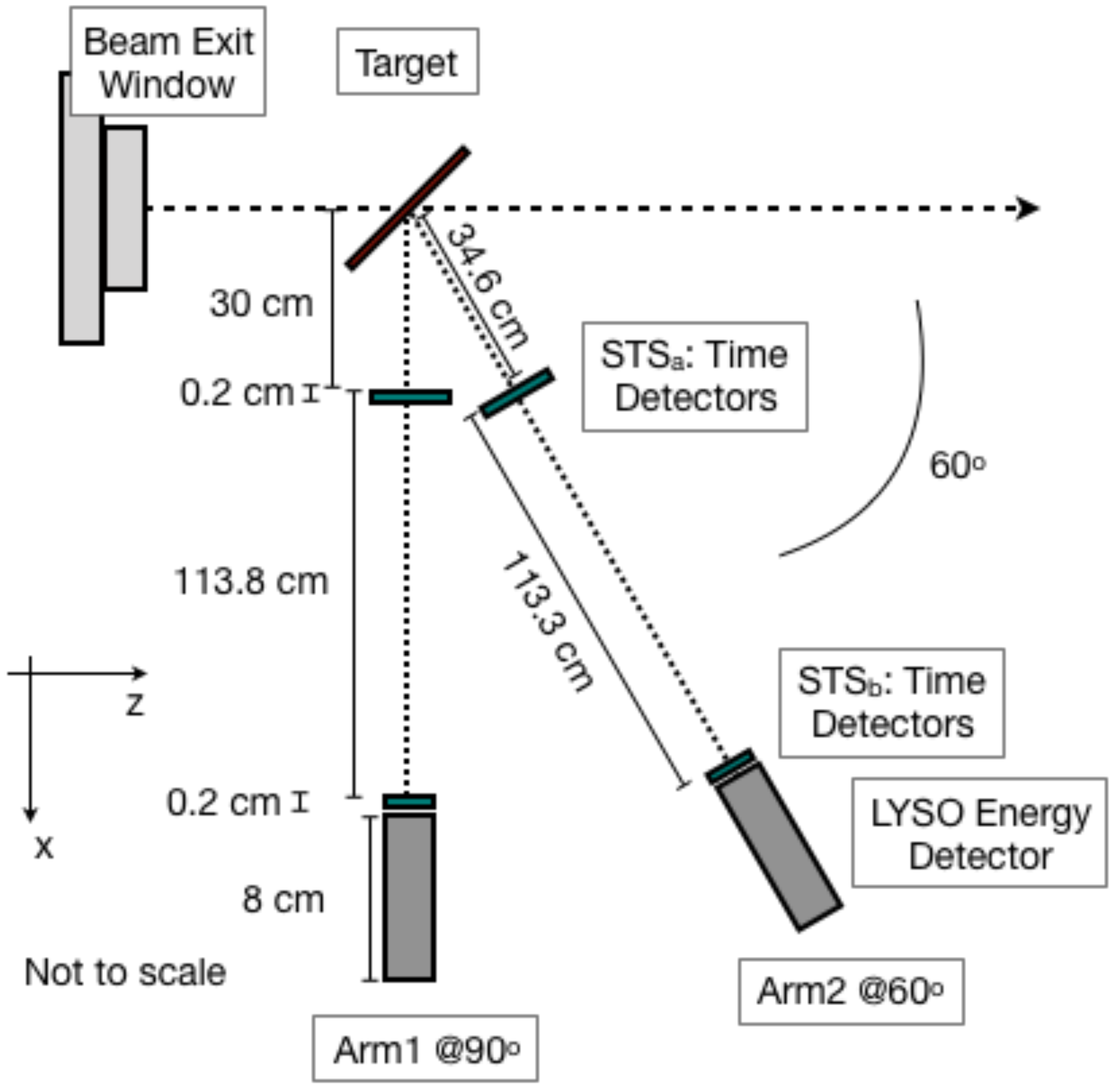

FIG. 1. Sketch of the experimental setup (not to scale)[1].

Many references to the previous published paper [1].

Section II: Methods

II. METHODS

The differential cross section computed as a function of the fragment kinetic energy at production (E_k) and measured at $\theta = 60°, 90°$ is defined as:

$$\frac{1}{\Delta\Omega}\frac{d\sigma}{dE_k}({}^{A}_{Z}X) = \frac{1}{\Delta\Omega}\frac{N_{{}^{A}_{Z}X}(E_k)}{N_Y\ \Delta E_k\ N_{^{12}C}\ \epsilon(E_k)}. \quad (1)$$

$N_{{}^{A}_{Z}X}(E_k)$ is the number of fragments with a specific atomic number Z and mass number A, in each kinetic energy bin E_k; $\Delta\Omega$ is the solid angle of the fragments at production seen and reconstructed by the LYSO detector; N_Y is the number of scattering centers per unit surface; ΔE_k is the fragment kinetic energy bin size; $N_{^{12}C}$ is the number of incoming carbon ions and $\epsilon(E_k)$ is the total efficiency.

$\Delta\Omega$ has been computed by means of the MC simulation, taking into account the spatial distribution of the beam and the multiple scattering underwent by fragments before reaching the LYSO detector. The number of scattering centres in a Y target per unit surface is defined as:

To compute the Differential Cross Section, above the normalization factors:

- **Evaluate the yield of fragments with specific Z and A as a function of the production kinetic energy of the fragments**
- **Evaluate the total efficiency as a function of the production kinetic energy of the fragments**

$$\epsilon(E_k) = \epsilon_{Rec} \cdot \epsilon_{PID} \cdot \epsilon_{DT}$$

Section II: Methods

II. METHODS

The differential cross section computed as a function of the fragment kinetic energy at production (E_k) and measured at $\theta = 60°, 90°$ is defined as:

$$\frac{1}{\Delta\Omega}\frac{d\sigma}{dE_k}({}^A_ZX) = \frac{1}{\Delta\Omega}\frac{N_{{}^A_ZX}(E_k)}{N_Y\ \Delta E_k\ N_{^{12}C}\ \epsilon(E_k)}\ . \qquad (1)$$

$N_{{}^A_ZX}(E_k)$ is the number of fragments with a specific atomic number Z and mass number A, in each kinetic energy bin E_k; $\Delta\Omega$ is the solid angle of the fragments at production seen and reconstructed by the LYSO detector; N_Y is the number of scattering centers per unit surface; ΔE_k is the fragment kinetic energy bin size; $N_{^{12}C}$ is the number of incoming carbon ions and $\epsilon(E_k)$ is the total efficiency.

$\Delta\Omega$ has been computed by means of the MC simulation, taking into account the spatial distribution of the beam and the multiple scattering underwent by fragments before reaching the LYSO detector. The number of scattering centres in a Y target per unit surface is defined as:

A. Fragment Identification

The number of specific fragments, $N_{{}^A_ZX}$ as a function of E_k, *i.e.* the fragment kinetic energy at production, is evaluated following the equation:

$$N_{{}^A_ZX}(E_k) = \boldsymbol{U} \cdot (N_{{}^A_ZX}(E_k^m) \cdot p(E_k^m)) \qquad (4)$$

where $\boldsymbol{U}$ is the unfolding matrix (see sec. II A 1), $p(E_k^m)$ is the *purity* (see eq. 5), $N_{{}^A_ZX}(E_k^m)$ is the number of ${}^A_ZX$ fragment as a function of the measured kinetic energy:

$$E_k^m = m_i c^2 \cdot (\gamma_i - 1);$$

with

$$\gamma_i = (1 - \beta_i^2)^{-1/2} \quad , \quad \beta_i = L/(ToF_i \cdot c).$$

1. Unfolding of measured kinetic energy

After the *purity* correction, to obtain the number of ${}^A_ZX$ fragment as a function of the kinetic energy of the fragment at production ($N_{{}^A_ZX}(E_k)$ in eq. 4), an unfolding technique, based on the *RooUnfoldBayes* method of the RooUnfold package[17] based on the ROOT software[18], has been applied to the measured kinetic energy spectrum, due to the fact that a fragment loses energy before exiting the target and in air before being detected. The

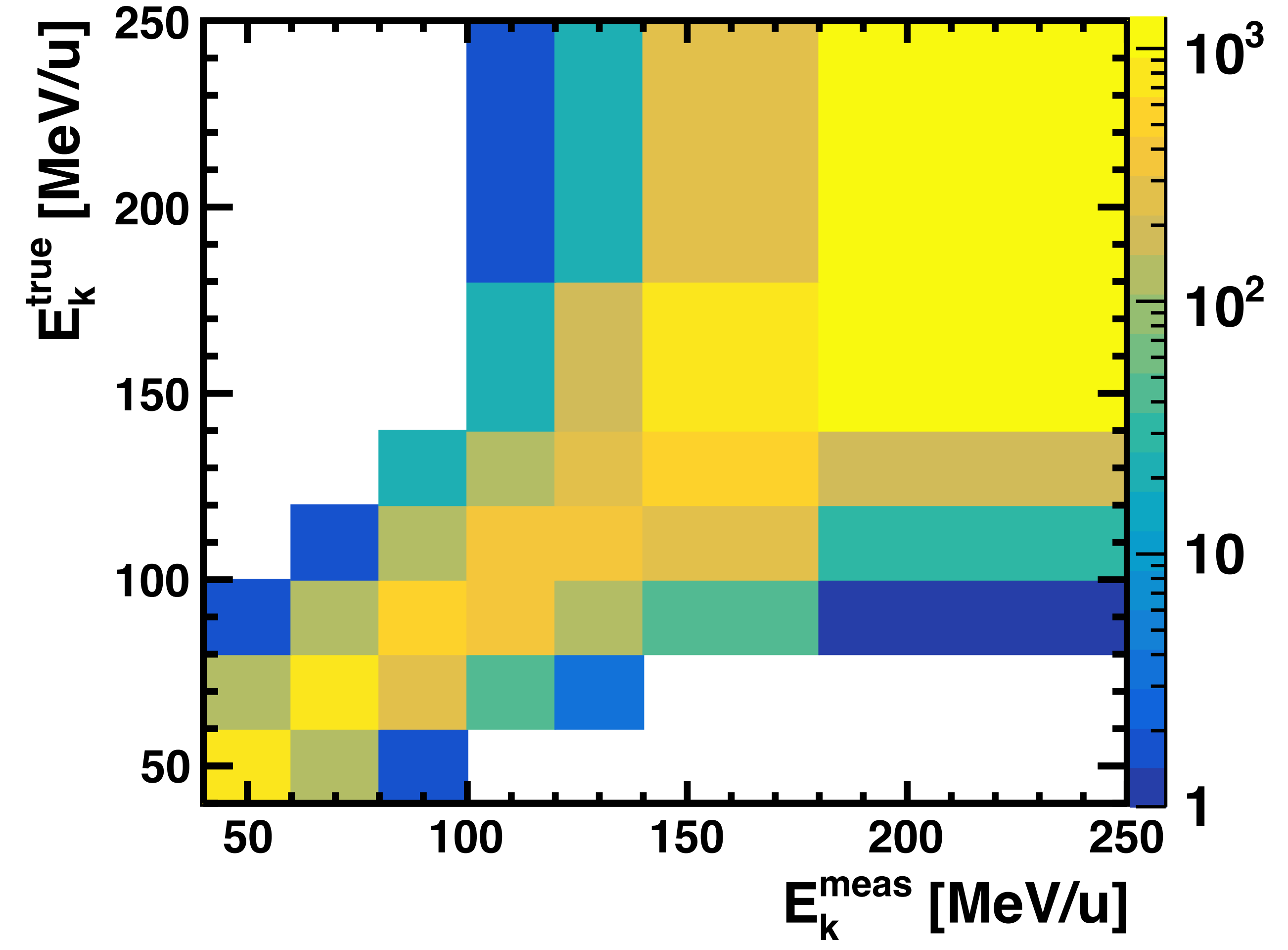

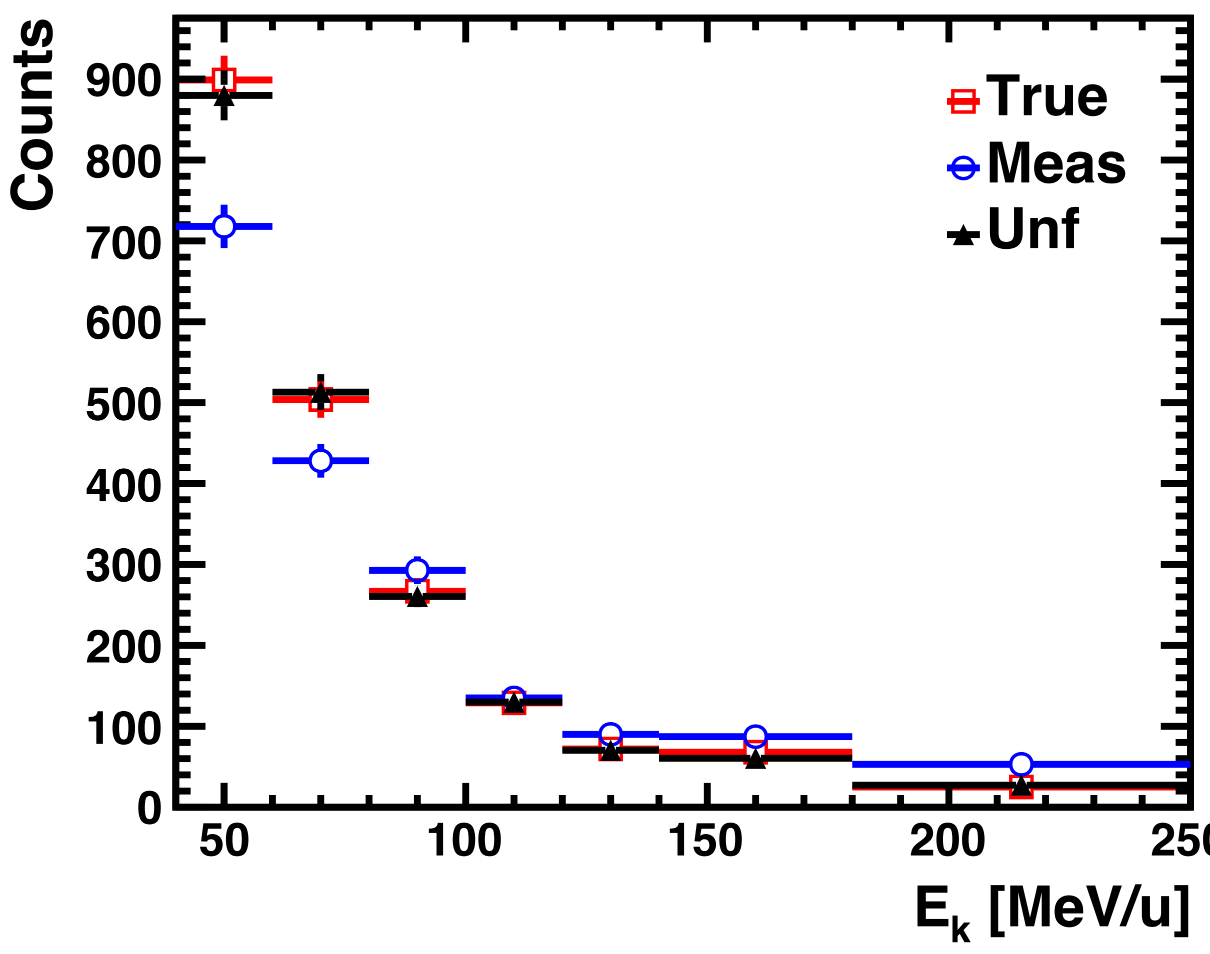

II. Methods

II.A Fragment Identification (refs to [1])

II.A.1 Unfolding of measured kinetic energy

Section II: Methods

B. Efficiency Evaluation

1. Reconstruction Efficiency

The reconstruction efficiency is the convolution of geometrical, trigger and detection efficiencies. It has been computed as a function of the fragment kinetic energy at production, following the equation:

$$\epsilon_{Rec}(E_k) = \frac{N^{recoMC}_{^A_ZX}(E_k)_{TE}}{N^{trueMC}_{^A_ZX}(E_k)_{\Delta\Omega}} \tag{6}$$

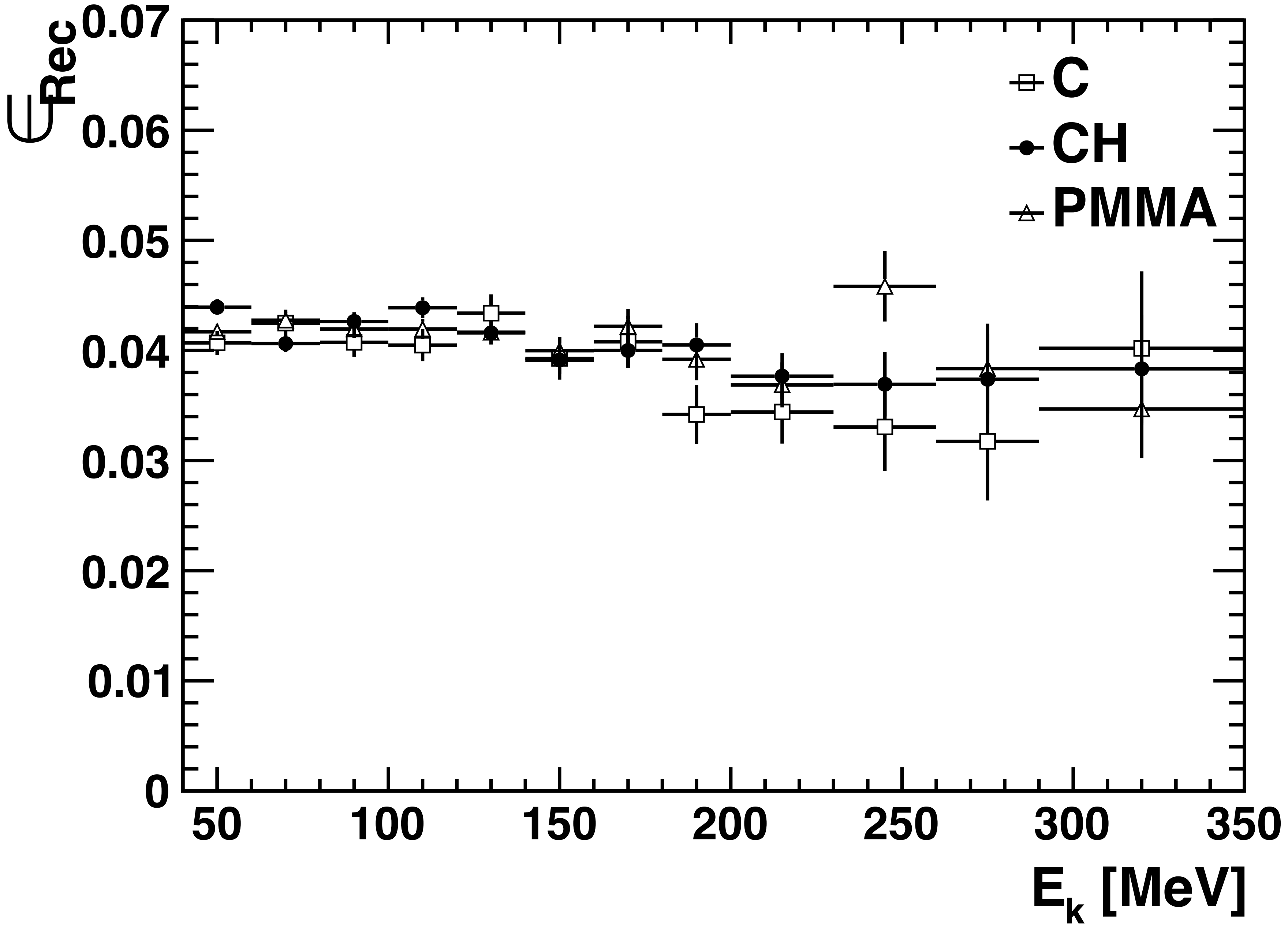

2. Particle Identification Efficiency

The particle identification efficiency (ϵ_{PID}) has been computed as a function of the reconstructed ^A_ZX fragment kinetic energy at production, with the following equation:

$$\epsilon_{PID}(E_k) = \frac{N^{recoMC}_{^A_ZX}(E_k)_{PID}}{N^{recoMC}_{^A_ZX}(E_k)_{TE}} \tag{7}$$

with $N^{recoMC}_{^A_ZX}(E_k)_{PID}$ is the number of fragment MC reconstructed in Z and A after the particle identification selection (see sec. II A), implemented as it is in experimental data, while $N^{recoMC}_{^A_ZX}(E_k)_{TE}$ is the same as the numerator of $\epsilon_{Rec}(E_k)$ (see sec. II B 1). In Table II

- II. Methods
  - II.A Fragment Identification
    - II.A.1 Unfolding
  - II.B Efficiency Evaluation
    - II.B.1 Reconstruction Efficiency
    - II.B.2 PID Efficiency

Section II: Methods

C. Systematic error evaluation

A crucial aspect in the evaluation of the results (see sec. III) is the assessment of the systematic error, that, in this analysis, is computed as a function of the fragment kinetic energy at production. The systematic error of the cross section measurement (as defined in eq. 1) is the root sum square of the systematic uncertainty sources listed below:

1. Unfolding procedure (sys_{unf})
2. $\Delta\Omega$ evaluation from MC simulation ($sys_{\Delta\Omega}$).
3. Particle identification selections (sys_{PID})
4. Evaluation of the number of incoming ions $N_{^{12}C}$ (relative systematics 4% - see sec. II)

II. Methods

- **II.A Fragment Identification**
  - **II.A.1 Unfolding**
- **II.B Efficiency Evaluation**
  - **II.B.1 Reconstruction Efficiency**
  - **II.B.2 PID Efficiency**
- **II.C Systematic Error Evaluation**

Section III: Results

III. RESULTS

The results on the differential cross section normalized to the solid angle (DCS in the following figures) of protons detected at 90° and 60°, produced by the nuclear fragmentation of ^{12}C ion beams of 115 - 351 MeV/u kinetic energy impinging over composite targets of PMMA, C and CH, computed as described by eq. 1, are shown as red squares, respectively, in Figs. 4 - 9. The statistical error (cross) and systematic error (empty square) on experimental data are shown as separate contributions. We also show the energy integrated values of the cross section normalized to the solid angle (CS in the following figures) as a function of the primary beam energy for the three targets (PMMA - left panel, C - middle panel, CH - right panel), for protons (p), deuterons (d) and tritons (t), detected at 90° (Fig. 10) and 60° (Fig. 11). The FLUKA MC prediction is superimposed to the experimental data as blue dots in all figures. Numerical values are reported in the tables shown in Appendix A. In the case of protons, low statistics kinetic energy bins are not included in tables.

The MC prediction results on differential cross section are computed with the following formula:

$$\frac{1}{\Delta\Omega}\frac{d\sigma^{trueMC}}{dE_k}({}^{A}_{Z}X) = \frac{1}{\Delta\Omega}\frac{N^{trueMC}_{{}^{A}_{Z}X}(E_k)_{\Delta\Omega}}{N_Y\ \Delta E_k\ N^{MC}_{^{12}C}} \qquad (8)$$

- **Differential Cross Section in Energy of protons**
- **Integral Cross Section of protons, deuterons and tritons (60º)**

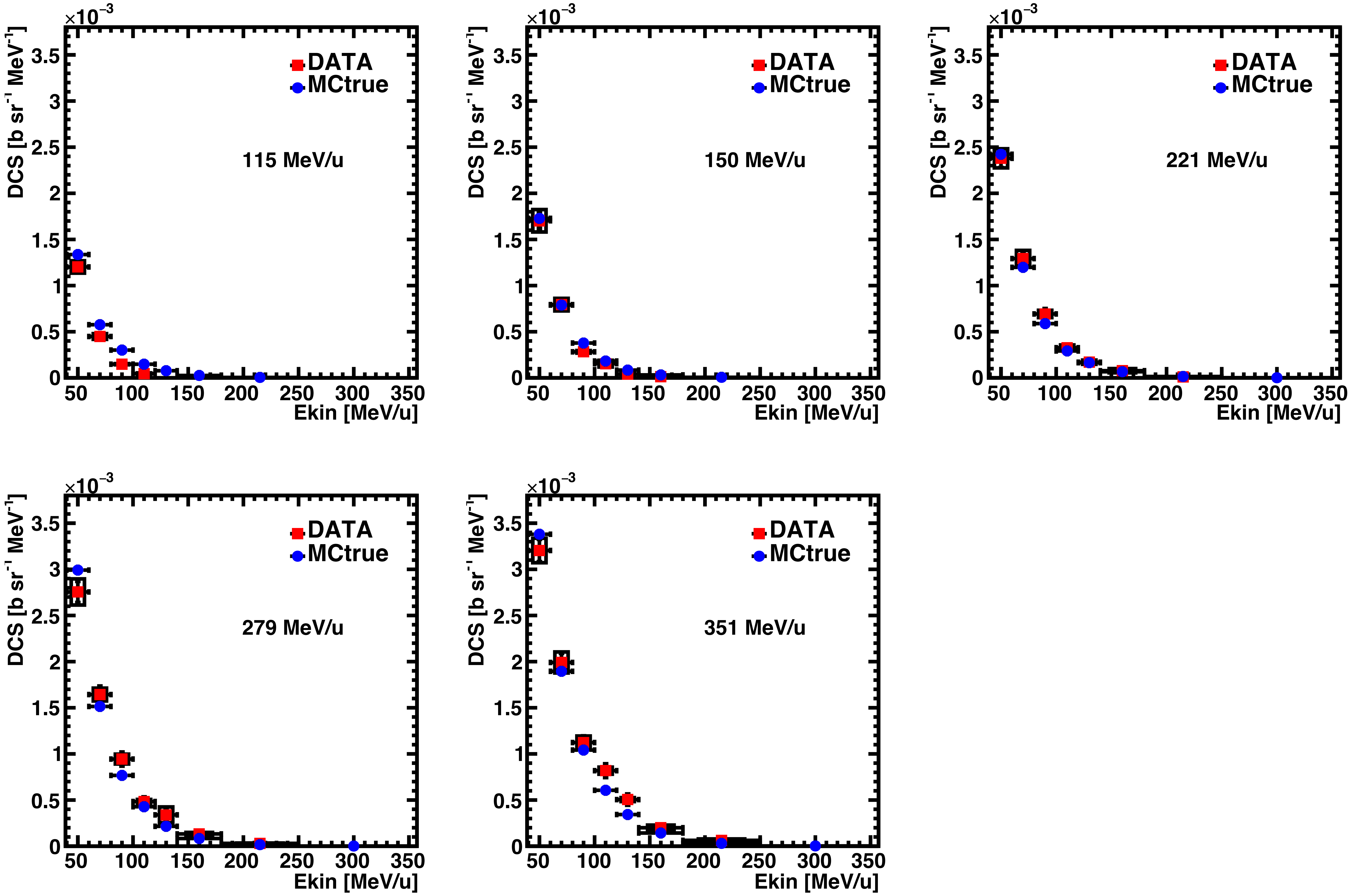

FIG. 4. Differential cross section in energy normalized to solid angle as a function of kinetic energy for proton fragments detected at 90°, produced in the nuclear interaction of 115-351 MeV/u carbon ion beam with a PMMA target. The statistical error (cross) and systematic error (empty square) on experimental data are shown as separate contributions.

Section III: Results

III. RESULTS

The results on the differential cross section normalized to the solid angle (DCS in the following figures) of protons detected at 90° and 60°, produced by the nuclear fragmentation of ^{12}C ion beams of 115 - 351 MeV/u kinetic energy impinging over composite targets of PMMA, C and CH, computed as described by eq. 1, are shown as red squares, respectively, in Figs. 4 - 9. The statistical error (cross) and systematic error (empty square) on experimental data are shown as separate contributions. We also show the energy integrated values of the cross section normalized to the solid angle (CS in the following figures) as a function of the primary beam energy for the three targets (PMMA - left panel, C - middle panel, CH - right panel), for protons (p), deuterons (d) and tritons (t), detected at 90° (Fig. 10) and 60° (Fig. 11). The FLUKA MC prediction is superimposed to the experimental data as blue dots in all figures. Numerical values are reported in the tables shown in Appendix A. In the case of protons, low statistics kinetic energy bins are not included in tables.

The MC prediction results on differential cross section are computed with the following formula:

$$\frac{1}{\Delta\Omega}\frac{d\sigma^{trueMC}}{dE_k}(^A_ZX) = \frac{1}{\Delta\Omega}\frac{N^{trueMC}_{^A_ZX}(E_k)_{\Delta\Omega}}{N_Y\ \Delta E_k\ N^{MC}_{^{12}C}} \quad (8)$$

Tables reporting DCS and CS results are presented in Appendix A

Appendix A: Double Differential Cross Section Tables

E^p_{kin} [MeV/u]	$\frac{d\sigma^{MC}_{true}}{dE_k}$	$\frac{d\sigma^{data}}{dE_k}$	stat^{data}	sys^{data}
90°	$\cdot 10^{-4}$ [b/sr/MeV]	$\cdot 10^{-4}$ [b/sr/MeV]	[%]	[%]
40 - 60	13.4 ± 0.1	12.0 ± 0.7 ± 0.7	5	6
60 - 80	5.76 ± 0.09	4.5 ± 0.4 ± 0.3	9	7
80 - 100	3.01 ± 0.06	1.48 ± 0.20 ± 0.06	13	4
100 - 120	1.48 ± 0.04	0.46 ± 0.08 ± 0.08	18	17
120 - 140	0.77 ± 0.03	-	-	-
140 - 180	0.26 ± 0.01	-	-	-
180 - 250	0.046 ± 0.004	-	-	-
60°	$\cdot 10^{-4}$ [b/sr/MeV]	$\cdot 10^{-4}$ [b/sr/MeV]	[%]	[%]
40 - 60	82.0 ± 0.3	79 ± 2 ± 4	2	5
60 - 80	49.8 ± 0.3	57 ± 2 ± 2	3	4
80 - 100	24.7 ± 0.2	29 ± 1 ± 2	4	6
100 - 120	11.2 ± 0.1	12.9 ± 0.8 ± 0.6	6	5
120 - 140	5.69 ± 0.09	8.4 ± 0.8 ± 0.5	9	5
140 - 160	2.97 ± 0.07	5.8 ± 0.8 ± 1.2	14	21
160 - 180	1.78 ± 0.05	2.0 ± 0.3 ± 0.6	15	31
180 - 200	0.95 ± 0.04	1.9 ± 0.5 ± 0.7	28	36
200 - 230	0.48 ± 0.02	0.8 ± 0.2 ± 0.2	29	22
230 - 260	0.19 ± 0.01	1.7 ± 1.6 ± 0.3	95	21
260 - 290	0.078 ± 0.009	-	-	-
290 - 350	0.026 ± 0.004	-	-	-

TABLE III. Differential cross section in kinetic energy bins at production (E^p_{kin}) of protons produced by 115 MeV/u ^{12}C ion beam impinging on a PMMA target, detected at 90° (top panel) and 60° (bottom panel). The production cross section from the FLUKA Monte Carlo simulation (*MC true*) is listed alongside the experimental cross section (*data*), with the relative statistical and systematic data uncertainties reported as percentage in the last two columns.

Section IV: Discussion and Conclusions

IV. DISCUSSION AND CONCLUSIONS

This work is devoted to the study of the emission of nucleons and light charged fragments at large polar angle in ^{12}C collisions in the energy range used in particle therapy. The main aim is to provide data to benchmark the models used for specific tasks, as those concerning range monitoring in ion therapy by means of the detection of light nuclear fragments emitted b other wor measured than ref.[1] angles (60

Comparison with already published data for proton fragments from graphite target

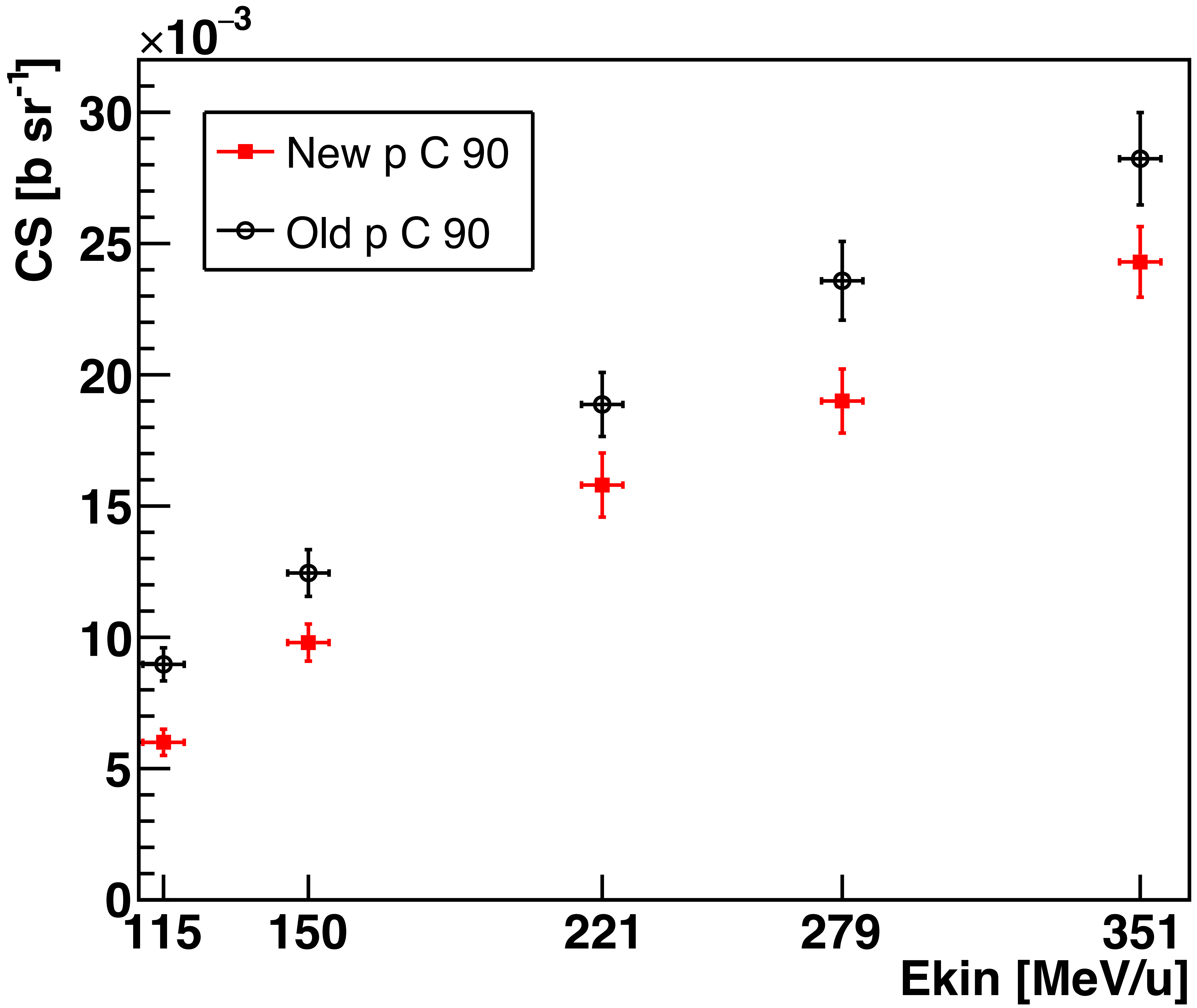

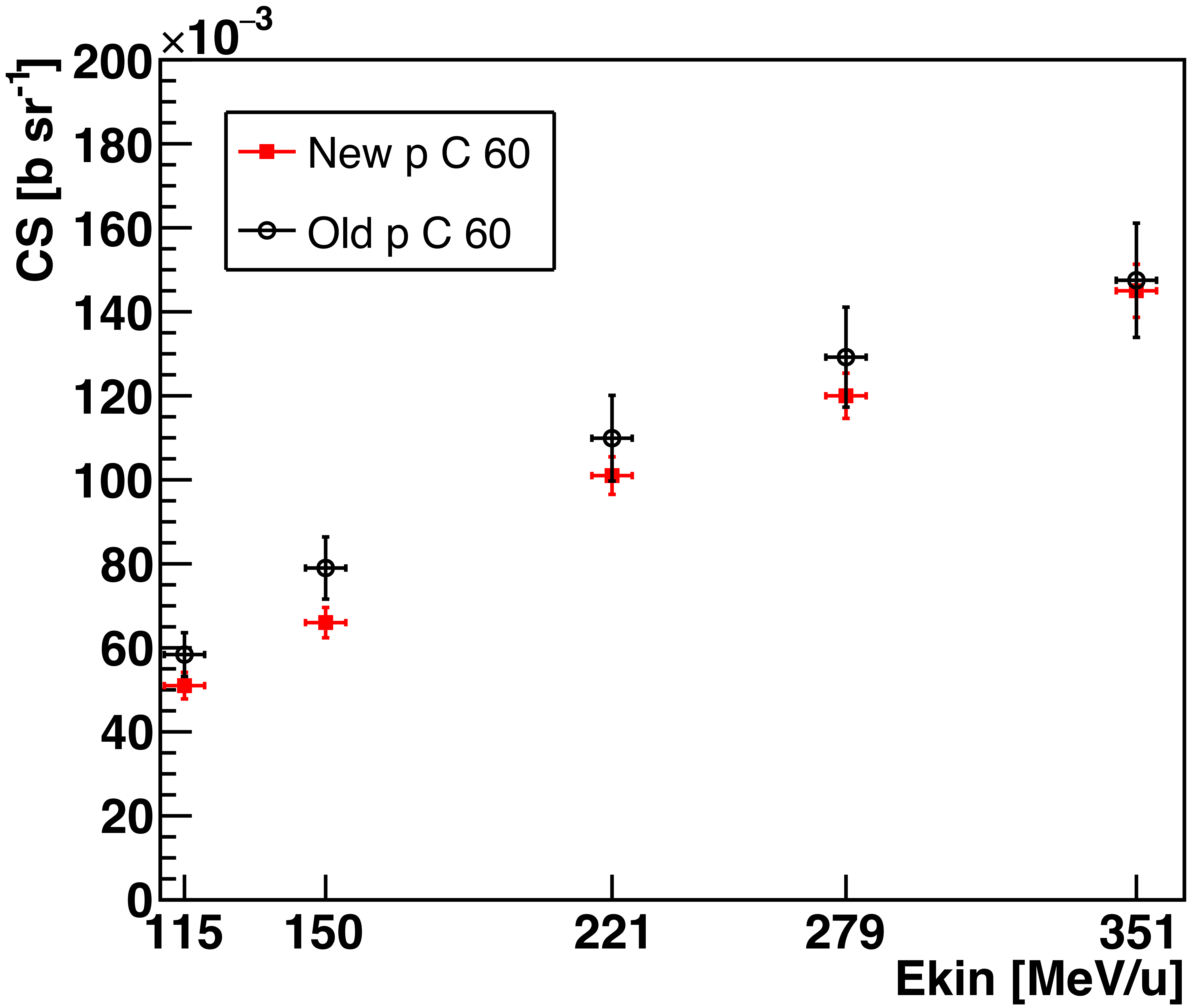

Section IV: Discussion and Conclusions

IV. DISCUSSION AND CONCLUSIONS

This work is devoted to the study of the emission of nucleons and light charged fragments at large polar angle in ^{12}C collisions in the energy range used in particle therapy. The main aim is to provide data to benchmark the models used for specific tasks, as those concerning range monitoring in ion therapy by means of the detection of light nuclear fragments emitted by the interaction of the therapeutic beam in the patient[5,19,20]. There have been other works in the past where data on yie
measured[21–24], but no cross section measure
than ref.[1]. In the present work, the differen
angles (60 and 90 degrees) from the nuclear

Thanks to Giuseppe Battistoni

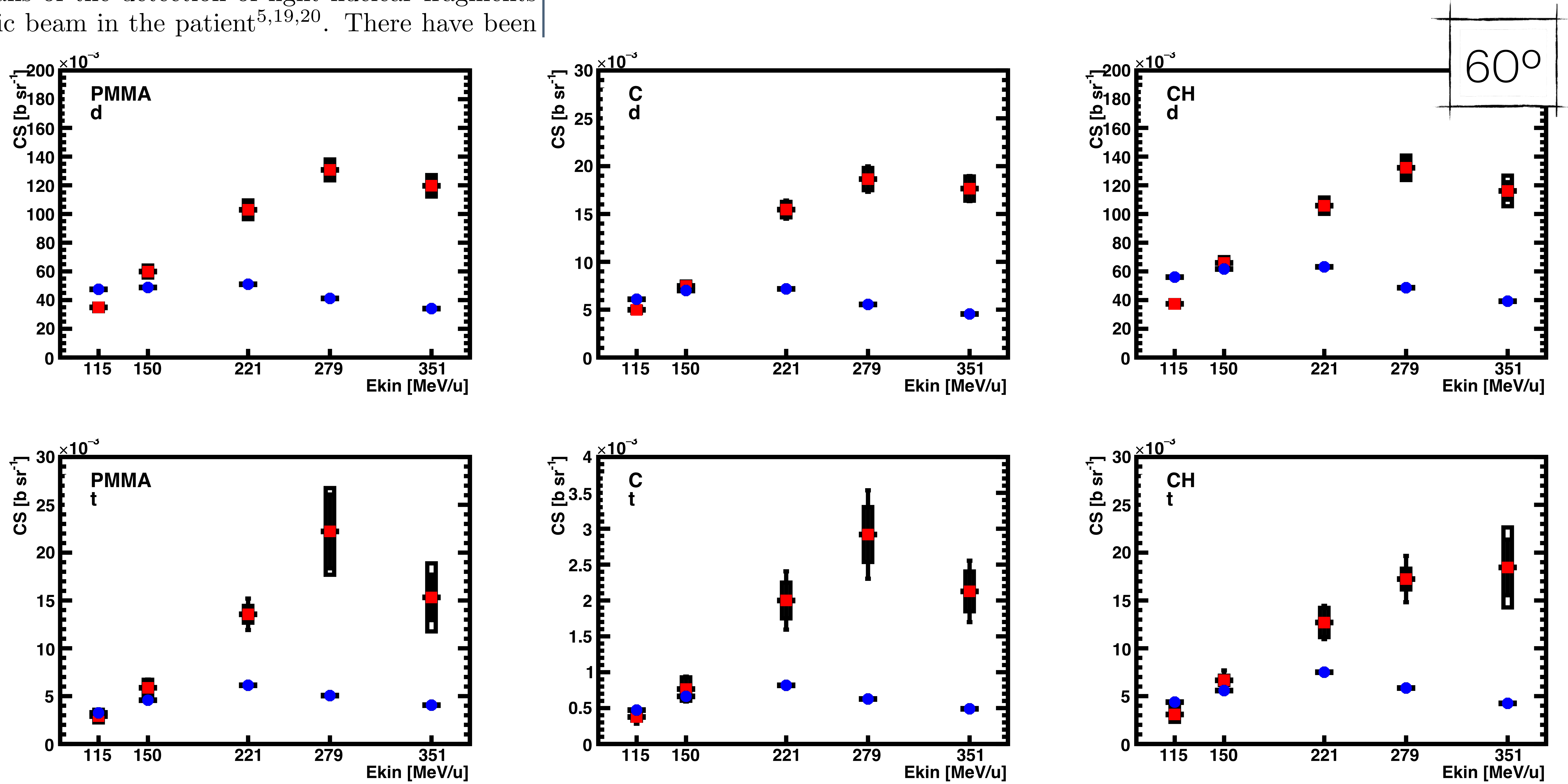

The disagreement of integral CS between data (red) and MC (blue) for *d* and *t* could be explained by the MC models that are not “well tested” at FOOT energies => confirmed by A. Ferrari (FLUKA Dad)

Cross Section Measurements of Large Angle Fragments Production in the Interaction of Carbon Ion Beams with Thin Targets

Y. Dong,[1] I. Mattei,[1] A. Alexandrov,[2] B. Alpat,[3] G. Ambrosi,[3] S. Argirò,[4,5] M. Barbanera,[3] N. Bartosik,[5] G. Battistoni,[1] M.G. Bisogni,[6,7] V. Boccia,[8,2] F. Cavanna,[5] P. Cerello,[5] E. Ciarrocchi,[6,7] A. De Gregorio,[9,10] G. De Lellis,[8,2] A. Di Crescenzo,[8,2] B. Di Ruzza,[11] M. Dondi,[12,13] M. Donetti,[14,5] M. Durante,[8,15] R. Faccini,[9,10] V. Ferrero,[5] C. Finck,[16] E. Fiorina,[5] M. Francesconi,[2] M. Franchini,[12,13] G. Franciosini,[17,10] G. Galati,[18] L. Galli,[7] M. Ionica,[3] A. Iuliano,[8,2] K. Kanxheri,[3,19] A.C. Kraan,[7] C. La Tessa,[20,21] A. Lauria,[8,2] E. Lopez Torres,[22,5] M. Magi,[17,10] A. Manna,[13,12] M. Marafini,[23,10] M. Massa,[7] C. Massimi,[12,13] A. Mengarelli,[13] A. Mereghetti,[14] T. Minniti,[24,25] A. Moggi,[7] M.C. Montesi,[2,26] M.C. Morone,[24,25] M. Morrocchi,[6,7] S. Muraro,[1] N. Pastrone,[5] V. Patera,[17,10] F. Peverini,[3,19] F. Pennazio,[5] C. Pisanti,[12,13] P. Placidi,[3,27] M. Pullia,[14] L. Ramello,[5,28] C. Reidel,[15] R. Ridolfi,[13,12] L. Sabatini,[29] L. Salvi,[3,19] C. Sanelli,[29] A. Sarti,[17,10] O. Sato,[30] S. Savazzi,[14] L. Scavarda,[31] A. Schiavi,[17,10] C. Schuy,[15] E. Scifoni,[21] L. Servoli,[3] G. Silvestre,[3] M. Sitta,[5,32] R. Spighi,[13] E. Spiriti,[29] L. Testa,[9,7] V. Tioukov,[2] S. Tomassini,[29] F. Tommasino,[33,21] M. Toppi,[17,10] A. Trigilio,[29] G. Traini,[10] G. Ubaldi,[12,13] A. Valetti,[4,5] M. Vanstalle,[16] U. Weber,[15] R. Zarrella,[12,13] A. Zoccoli,[12,13] and M. Villa[12,13]

1) *INFN Section of Milano, Milano, Italy*
2) *INFN Section of Napoli, Napoli, Italy*
3) *INFN Section of Perugia, Perugia, Italy*
4) *University of Torino, Department of Physics, Torino, Italy*
5) *INFN Section of Torino, Torino, Italy*
6) *University of Pisa, Department of Physics, Pisa, Italy*
7) *INFN Section of Pisa, Pisa, Italy*
8) *University of Napoli, Department of Physics "E. Pancini", Napoli, Italy*
9) *University of Rome La Sapienza, Department of Physics, Rome, Italy*
10) *INFN Section of Roma 1, Rome, Italy*
11) *University of Foggia, Foggia, Italy*
12) *University of Bologna, Department of Physics and Astronomy, Bologna, Italy*
13) *INFN Section of Bologna, Bologna, Italy*
14) *CNAO Centro Nazionale di Adroterapia Oncologica , Pavia, Italy*
15) *Biophysics Department, GSI Helmholtzzentrum für Schwerionenforschung, Darmstadt, Germany*
16) *Université de Strasbourg, CNRS, IPHC UMR 7871, F-67000 Strasbourg, France*
17) *University of Rome La Sapienza, Department of Scienze di Base e Applicate per l'Ingegneria (SBAI), Rome, Italy*
18) *University of Bari, Department of Physics, Bari Italy*
19) *University of Perugia, Department of Physics and Geology, Perugia, Italy*
20) *University of Miami, Radiation Oncology, Miami, FL, United State*
21) *Trento Institute for Fundamental Physics and Applications, Istituto Nazionale di Fisica Nucleare (TIFPA-INFN), Trento, Italy*
22) *CEADEN, Centro de Aplicaciones Tecnologicas y Desarrollo Nuclear, Havana, Cuba*
23) *Museo Storico della Fisica e Centro Studi e Ricerche Enrico Fermi, Rome, Italy*
24) *University of Rome Tor Vergata, Department of Physics, Rome, Italy*
25) *INFN Section of Roma Tor Vergata, Rome, Italy*

Important Dates

Deadline to receive feedbacks and comments: **22 of December**

Submit to PRC: **24 of December**

Thank you for the Attention

Backup

Section II: Methods

II.A Fragment Identification:

very same procedure described in the 2021 published paper.
Same distributions used as well as same selection "bands" to select in charge (Z_{id}) and mass (A_{id}).